ISSN 1063-7834, Physics of the Solid State, 2010, Vol. 52, No. 8, pp. 1664–1672. © Pleiades Publishing, Ltd., 2010.
Original Russian Text © B.A. Belyaev, A.V. Izotov, An.A. Leksikov, 2010, published in Fizika Tverdogo Tela, 2010, Vol. 52, No. 8, pp. 1549–1556.

MAGNETISM AND FERROELECTRICITY

Micromagnetic Calculation of the Equilibrium Distribution of Magnetic Moments in Thin Films

B. A. Belyaev[a,*], A. V. Izotov[b], and An. A. Leksikov[a]

[a] *Kirensky Institute of Physics, Siberian Branch, Russian Academy of Sciences, Akademgorodok 50, Krasnoyarsk, 660036 Russia*

* *e-mail: belyaev@iph.krasn.ru*

[b] *Siberian Federal University, pr. Svobodnyĭ 79, Krasnoyarsk, 660041 Russia*

Received October 14, 2009

Abstract—A new approach has been proposed for determining an equilibrium configuration of magnetic moments in condensed matter in terms of its discrete model. The solution to this problem is reduced to a system of linear inhomogeneous equations with undetermined Lagrange multipliers. The possibility of numerically solving these systems has been shown using a modified power method. The efficiency of the method has been demonstrated for the model of a thin magnetic film with a nonuniform distribution of the uniaxial magnetic anisotropy over the area. The dependence of the coercive force on the uniaxial anisotropy of nanocrystallites, their exchange interaction, and other parameters of samples has been investigated.

DOI: 10.1134/S1063783410080160

1. INTRODUCTION

In recent years, an increased interest expressed in nanomaterials, including magnetic nanomaterials [1], has been motivated by great potential possibilities of their practical application. Progress in computational capabilities of modern computers allows one to investigate properties of these materials by using the numerical solution to problems for models that reflect a microdiscrete structure of media. The results of numerical investigations are especially valuable in the cases where the derivation of the analytical solution for a system is almost impossible. These facts have stimulated a rapid increase not only in the number of works devoted to the study of properties of nanomaterials with the use of their micromagnetic models [2–5] but also in the number of works devoted to the development of models themselves and effective methods for their calculations [6–8]. In particular, the model based on the so-called discrete-dipole approximation has been widely used in numerical simulation of magnetic media. According to this model, the discrete medium is treated as a set of magnetic dipoles (moments), which, depending on the level of detail and the problem to be solved, can be considered to mean individual spins and magnetic moments of cells into which the medium is separated. In the latter case, the cells can be considered to be nanoparticles themselves, microcrystallites, or regions organized in a different manner, within which the magnetic moment is assumed to be uniform.

In the framework of the discrete-dipole model, the solution to a number of problems leads to an important problem regarding the determination of the equilibrium state or equilibrium configuration of the distribution of magnetic moments. These are problems associated with the study of static magnetic characteristics of media, for example, the investigation of the domain structure [9] or the calculation of hysteresis loops [10]. Moreover, these are problems regarding the study of their dynamic properties, such as the determination of normal modes of magnetic oscillations of nanoparticles [7, 8] or the calculation of the absorption spectrum of the spin-wave resonance [11]. There exist several different approaches that make it possible to determine the equilibrium configuration of magnetic moments [12], and each approach, as a rule, is used for solving a particular class of problems. For example, one of the approaches is based on the integration of the system of Landau–Lifshitz–Hilbert differential equations by the Runge–Kutta method for each subsequent configuration of magnetic moments beginning with a randomly specified configuration. This approach is most general and implemented in the known program packages on the micromagnetic simulation, such as OOMMF [13] and magpar [14], which allow one to investigate static and dynamic properties of systems. However, this approach to the determination of the equilibrium state has a number of computational disadvantages. First, the approach is characterized by a relatively low rate, because the entire evolution of the magnetic system in time is calculated in order to obtain the final distribution of mag-

netic moments. Second, special measures should be undertaken in order to ensure constant dipole moments.

The next approach, which provides a means for determining configurations of magnetic moments that are sufficiently close to the ground equilibrium state of the system, is based on the Monte Carlo method. However, this approach requires a considerable computer time even for a relatively small number of dipoles in the model. One more approach is based on the minimization of the energy of the system under consideration by different methods, for example, the relaxation or gradient descent method. The presence of a large number of metastable states and nonlinearity of the system results in the fact that computational procedures are extremely unstable, can have a poor convergence, and even be divergent. The use of this approach is also limited by consideration of models with a relatively small number of elements.

Good results on the determination of the equilibrium configuration of the magnetic state of a system of particles is provided by the approach based on the relaxation of the system according to the behavior of its internal effective magnetic fields acting on each dipole. For this purpose, the local field at a specific magnetic dipole is calculated sequentially or in a random order and its new position is determined in accordance with the corresponding forces. The calculations are continued until the positions of all magnetic moments are stabilized. In the majority of cases, this method is more reliable and most rapid; however, situations of cycling of iterative calculations in the appearance of jumps between two unstable states are possible [12]. In essence, the method proposed in the present work is the generalization of the last approach. It should be noted that the method is free of many disadvantages, for example, possible cycling of calculations. Furthermore, the formulated problem regarding the determination of the equilibrium state of magnetic moments is reduced to the problem of linear algebra, which, in turn, makes it possible to apply effective numerical methods for a large number of interacting dipoles, including the use of sparse matrices and parallel calculations when solving large-scale problems on multiprocessor systems.

2. THEORETICAL BACKGROUND

Let us consider a ferromagnet as a discrete medium consisting of N identical magnetic dipoles $\boldsymbol{\mu}^{(i)}$ ($i = 1, 2, \ldots, N$), which uniformly fill the entire volume of the solid under investigation. We assume that the saturation magnetization M_s is constant. By designating the direction of the ith dipole as $\mathbf{M}^{(i)}$ and its volume as V_0 (i.e., $\boldsymbol{\mu}^{(i)} = M_s V_0 \mathbf{M}^{(i)}$, the expression for the free energy F of the system under consideration can be written in the form of the sum of the Zeeman energy F_z, the exchange interaction energy F_{ex}, the dipole–dipole interaction energy F_{dip}, and the uniaxial magnetic anisotropy energy F_a:

$$F = F_z + F_{ex} + F_{dip} + F_a,$$

$$F_z(\mathbf{M}^{(1)}, \mathbf{M}^{(2)}, \ldots, \mathbf{M}^{(N)}) = -M_s V_0 \mathbf{H} \sum_{i=1}^{N} \mathbf{M}^{(i)},$$

$$F_{ex}(\mathbf{M}^{(1)}, \mathbf{M}^{(2)}, \ldots, \mathbf{M}^{(N)}) = JV_0 \sum_{i=1}^{N} \sum_{j=1}^{Ni} (1 - \mathbf{M}^{(i)}\mathbf{M}^{(j)}),$$

$$F_{dip}(\mathbf{M}^{(1)}, \mathbf{M}^{(2)}, \ldots, \mathbf{M}^{(N)}) \quad (1)$$

$$= \frac{M_s^2 V_0^2}{2} \sum_{i=1}^{N} \sum_{\substack{j=1 \\ j \neq i}}^{N} \left[\frac{\mathbf{M}^{(i)}\mathbf{M}^{(j)}}{r_{ij}^3} - \frac{3(\mathbf{M}^{(i)}\mathbf{r}^{(ij)})(\mathbf{M}^{(j)}\mathbf{r}^{(ij)})}{r_{ij}^5} \right],$$

$$F_a(\mathbf{M}^{(1)}, \mathbf{M}^{(2)}, \ldots, \mathbf{M}^{(N)}) = -V_0 \sum_{i=1}^{N} K_i (\mathbf{M}^{(i)}\mathbf{n}^{(i)})^2.$$

Here, $\mathbf{H}$ is the external magnetic field applied to the medium, J is the exchange interaction constant (in this case, the second sign of the sum over j in the exchange energy holds true only for the Ni nearest neighbors of the ith dipole), $\mathbf{r}^{(ij)}$ is the distance vector between the ith and jth dipoles, r_{ij} is the magnitude of this vector, K_i is the uniaxial magnetic anisotropy constant, and $\mathbf{n}^{(i)}$ is the unit vector coinciding with the direction of the easy magnetization axis.

The expression for the free energy can be represented with the use of the generalized interaction matrix, which is determined only by the internal properties of the magnetic medium under investigation. For this purpose, we initially introduce the effective dipole–dipole interaction tensor $\overleftrightarrow{A}_{ij}$:

$$\overleftrightarrow{A}_{ij} = \begin{cases} \overleftrightarrow{A}^{a}_{ii}, & i = j \\ \overleftrightarrow{A}^{ex}_{ij} + \overleftrightarrow{A}^{dip}_{ij}, & i \neq j, \end{cases}$$

$$\overleftrightarrow{A}^{ex}_{ij} = \frac{2J}{M_s} E,$$

$$\overleftrightarrow{A}^{dip}_{ij} = -M_s V_0 \frac{1}{r_{ij}^3} \left[E - \frac{3}{r_{ij}^2} \begin{pmatrix} r_x^{(ij)} \\ r_y^{(ij)} \\ r_z^{(ij)} \end{pmatrix} (r_x^{(ij)} \; r_y^{(ij)} \; r_z^{(ij)}) \right], \quad (2)$$

$$\overleftrightarrow{A}^{a}_{ii} = \frac{2K_i}{M_s}\begin{pmatrix} n_x^{(i)} \\ n_y^{(i)} \\ n_z^{(i)} \end{pmatrix}(n_x^{(i)}\ n_y^{(i)}\ n_z^{(i)}),$$

where E is the 3-by-3 unit matrix, $\overleftrightarrow{A}^{\mathrm{ex}}_{ij}$ are the components of the tensor describing the exchange interaction (between the ith and jth neighbors), $\overleftrightarrow{A}^{\mathrm{dip}}_{ij}$ are the components of the tensor describing the dipole–dipole (magnetostatic) interaction, and $\overleftrightarrow{A}^{a}_{ij}$ are the components of the tensor describing the anisotropy.

Then, the relationship for the free energy (1) within the terms independent of $\mathbf{M}^{(i)}$ can be written as follows:

$$F(\mathbf{M}^{(1)}, \mathbf{M}^{(2)}, \ldots, \mathbf{M}^{(N)}) = -M_s V_0 \sum_{i=1}^{N}\left[\mathbf{H}\mathbf{M}^{(i)} + \frac{1}{2}\sum_{j=1}^{N}\mathbf{M}^{(i)}\overleftrightarrow{A}_{ij}\mathbf{M}^{(j)}\right]. \quad (3)$$

By introducing the generalized interaction matrix A, the generalized dipole vector $\mathbf{x}$, and the external interaction vector $\mathbf{b}$ in the form

$$A = \begin{bmatrix} \overleftrightarrow{A}_{11} & \overleftrightarrow{A}_{12} & \ldots & \overleftrightarrow{A}_{1N} \\ \overleftrightarrow{A}_{21} & \overleftrightarrow{A}_{22} & \ldots & \overleftrightarrow{A}_{2N} \\ \ldots & \ldots & \ldots & \ldots \\ \overleftrightarrow{A}_{N1} & \overleftrightarrow{A}_{N2} & \ldots & \overleftrightarrow{A}_{NN} \end{bmatrix}, \quad \mathbf{x} = \begin{bmatrix} \mathbf{M}^{(1)} \\ \mathbf{M}^{(2)} \\ \ldots \\ \mathbf{M}^{N} \end{bmatrix}, \quad \mathbf{b} = \begin{bmatrix} \mathbf{H} \\ \mathbf{H} \\ \ldots \\ \mathbf{H} \end{bmatrix}, \quad (4)$$

we obtain the expression for the free energy in the matrix form

$$F(A, \mathbf{x}, \mathbf{b}) = -M_s V_0\left(\frac{1}{2}\mathbf{x}^T A\mathbf{x} + \mathbf{b}^T\mathbf{x}\right). \quad (5)$$

In this expression the prefix T indicates the transposition.

Therefore, in the framework of the approach under consideration, the simulated medium is described by the generalized matrix A, for which the components are determined by the properties of the medium itself and depend neither on the external conditions nor on the distribution of magnetic moments in it.

As is known, to an equilibrium configuration of the magnetic moment distribution there corresponds a minimum of the free energy, i.e., the equality of its variation to zero:

$$\delta F(\mathbf{M}^{(1)}, \mathbf{M}^{(2)}, \ldots, \mathbf{M}^{(N)}) = 0, \quad (6)$$

with the additional condition that the length of each dipole is constant

$$\mathbf{M}^{(i)2} = M_x^{(i)2} + M_y^{(i)2} + M_z^{(i)2} = \mathrm{const} = 1 \quad (i = 1, 2, \ldots, N). \quad (7)$$

It is evident that Eq. (7) decreases the number of independent variables in Eq. (6) from $3N$ to $2N$, on the one hand, and makes this equation nonlinear, on the other hand. In order to verify this fact, it is sufficient to choose an arbitrary component of the vector $\mathbf{M}^{(i)}$ and to substitute it into relationship (6). In this case, as was noted in Introduction, the methods based on the minimization of functional (1) with condition (7) find a limited use, because they are extremely unstable.

However, this problem can be solved in another manner based on the use of the undetermined Lagrange multiplier method. As a result, the necessary equilibrium condition can be written in the form of the system [15]

$$\frac{\delta}{\delta\mathbf{M}^{(k)}}\left[F + M_s V_0\frac{\nu_k}{2}\mathbf{M}^{(k)2}\right] = 0, \quad (8)$$

where $k = 1, 2, \ldots, N$, ν_k are constant Lagrange multipliers, and $\delta/\delta\mathbf{M}^{(k)}$ is the variational derivative, which, in our case, is equal to $\partial/\partial\mathbf{M}^{(k)}$.

By introducing the effective local magnetic field

$$\mathbf{H}^{\mathrm{eff}(k)} = -\frac{1}{M_s V_0}\frac{\delta F}{\delta\mathbf{M}^{(k)}} \quad (9)$$

system (8) transforms into the form

$$\mathbf{H}^{\mathrm{eff}(k)}(\mathbf{M}^{(1)}, \mathbf{M}^{(2)}, \ldots, \mathbf{M}^{(N)}) - \nu_k\mathbf{M}^{(k)} = 0. \quad (10)$$

The physical meaning of the last equations lies in the fact that each magnetic moment in the equilibrium state coincides in direction with the effective local magnetic field produced by both the external field and the effective fields associated with the anisotropy and the interaction of dipoles entering into the composition of the system under consideration. In this case, the proportionality coefficient ν_k provides the constancy of the length of magnetic moments.

Since the terms that enter into expression (1) for the free energy and describe different interaction types (except for the Zeeman energy) are quadratic forms with respect to the quantity $\mathbf{M}^{(i)}$, the system of equations (10) is linear. It should be noted that the only linear relationship in (1) that describes the interaction with the external magnetic field makes system (10)

inhomogeneous. In order to check this fact, we write the expression for the effective local magnetic field with allowance made for relationship (9) in the form

$$\mathbf{H}^{\text{eff}(k)}(\mathbf{M}^{(1)}, \mathbf{M}^{(2)}, \ldots, \mathbf{M}^{(N)}) = \mathbf{H} + \sum_{j=1}^{N} \overleftrightarrow{A}_{kj}\mathbf{M}^{(j)}. \quad (11)$$

We introduce the diagonal matrix $D = \text{diag}(\nu_1, \nu_1, \nu_1, \nu_2, \nu_2, \ldots, \nu_{3N})$ consisting of undetermined Lagrange multipliers. Then, with the use of the generalized matrix, the system of equations (10) can be represented in the matrix form

$$A\mathbf{x} - D\mathbf{x} = -\mathbf{b}. \quad (12)$$

This matrix equation can be solved using the developed numerical algorithms of linear algebra. As an example, we can describe the simplest algorithm that represents some modification of the power method used for solving the partial eigenvalue problem [16]. To accomplish this, we rewrite Eq. (12) in the form $D\mathbf{x} = A\mathbf{x} + \mathbf{b}$ and, by designating $\mathbf{y} = D\mathbf{x}$, obtain the iterative scheme

$$\begin{aligned} \mathbf{y}_{i+1} &= A\mathbf{x}_i + \mathbf{b}, \\ \mathbf{x}_{i+1} &= D_{i+1}^{-1}\mathbf{y}_{i+1}. \end{aligned} \quad (13)$$

In this case, the coefficients of the diagonal matrix D_{i+1}^{-1} are chosen in such a way as to provide the fulfillment of condition (7) and the calculations are continued until the components of the vector $\mathbf{x}$ are stabilized.

The necessary condition for the convergence and stability (including the absence of cycling) of this iterative process is a positive definiteness of the matrix A; i.e., when the quadratic form $\mathbf{x}^T A\mathbf{x}$ is larger than zero [16]. In our case, this can be always achieved by solving the equation $A'\mathbf{x} - D'\mathbf{x} = \mathbf{b}$ instead of the matrix equation (12), where $A' = A + \xi E$, $D' = D + \xi E$, and E is the unit matrix. By appropriately choosing the quantity $\xi > 0$, we obtain the positive-definite matrix A'.

It should be noted that this algorithm does not possess a fast convergence; nonetheless, the corresponding rate in the majority of cases can multiply exceed the rate of other methods. When the matrix A has a large dimension or is strongly sparse (for example, if the dipole–dipole interaction in the model is ignored or only partially takes into account), it is necessary to use other more effective algorithms.

3. RESULTS OF THE NUMERICAL SIMULATION

The efficiency of the proposed approach was verified for films that represented monolayers of magnetic nanoparticles with the dimension $n \times n$ and a random distribution of anisotropy axes. For comparison and evaluation of the reliability of the calculations, the model of the thin-film sample and the values of the parameters of nanoparticles forming the sample were taken from the work by Il'yushchenkov et al. [9], who obtained the equilibrium distribution of magnetic moments in the nickel film consisting of closely packed grains by the Monte Carlo method. In [9], the authors disregarded the dispersion of particle sizes and considered that the size of grains is equal to 2.5 nm; i.e., according to the estimates, the grain should contain ~600 atoms. The authors also assumed that the contact between particles is characterized by the presence of tunneling barriers, which leads to a weakening of the exchange interaction characterized by the effective exchange interaction constant J^{eff}. It was assumed that the particles have a saturation magnetization $M_s = 495$ G and a uniaxial magnetic anisotropy constant $K_u = 8 \times 10^5$ erg/cm^3. A comparison of our equilibrium distributions of magnetic moments in the samples under consideration [17] with the corresponding data obtained in [9] demonstrates good agreement at all ratios J^{eff}/K_u for a random distribution of anisotropy axes of nanoparticles not only in the plane of the sample but also in the space.

The developed approach to the determination of the ground state of the discrete model of the ferromagnet allows us not only to determine the equilibrium distribution of magnetic moments for any specified parameters of the structure under investigation but also to investigate the processes of its magnetization reversal. As an example, Fig. 1 shows the hysteresis loops for the monolayer cobalt film containing 50×50 crystallites 2.5 nm in size for one of the random distributions of the anisotropy axes in the plane according to the calculations for different angles φ of the orientation of the planar magnetizing field. In the calculations, it was assumed that the anisotropy field of the individual dipole is $H_k = 3.5$ kOe, its saturation magnetization is $M_s = 1250$ G, and the exchange interaction constant is $J = 10^8$ erg/cm^3. In this case, the dipole–dipole interaction was taken into account up to the distance equal to eight exchange correlation lengths R.

It can be seen from Fig. 1 that the coercive force and the shape of the hysteresis loops are determined, to a considerable, extent, by the direction of the constant magnetic field, for which the orientation angle was measured with respect to one of the sides of the

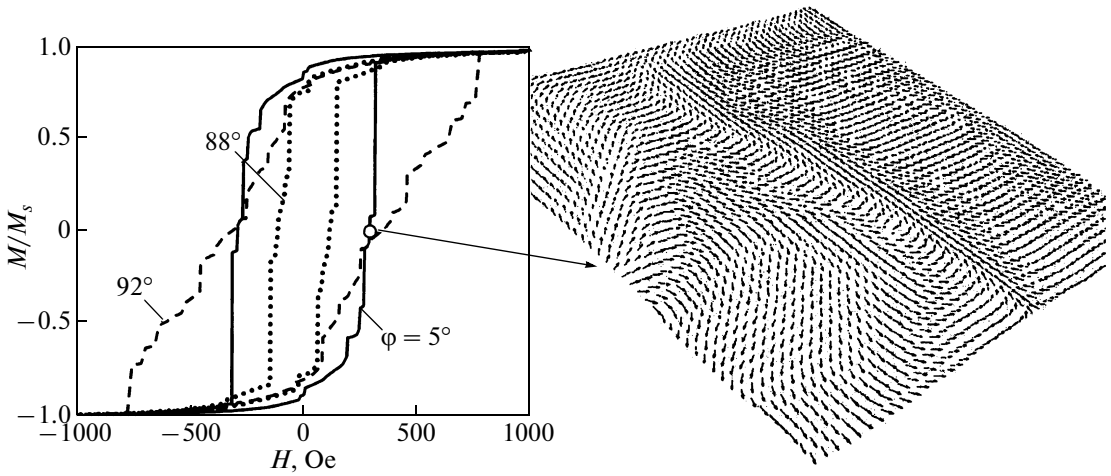

Fig. 1. Hysteresis loops of the structure with a random distribution of anisotropy axes of dipoles for different angles of the magnetic field orientation in the film with a dimension of 50 × 50. The equilibrium configuration of magnetic moments in the constant magnetic field $H = 250$ Oe is shown at the right.

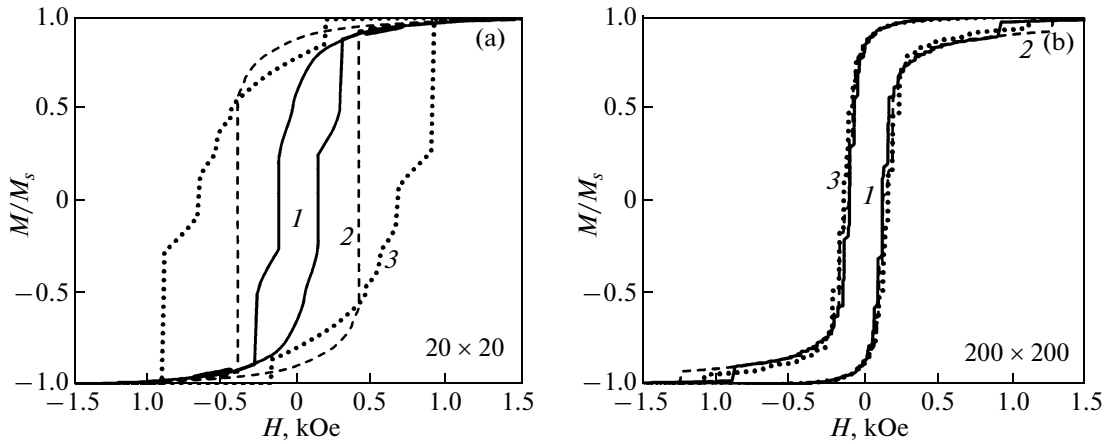

Fig. 2. Hysteresis loops constructed for three random distributions of anisotropy axes in the films with dimensions of (a) 20 × 20 and (b) 200 × 200 dipoles.

square sample. The presence of jumps in the hysteresis loops is associated with the overcoming of energy barriers, so that the heights and number of these energy barriers depend not only on a specific distribution of the anisotropy axes in the system of dipoles but also on the direction of the magnetization reversal field. The equilibrium distribution of magnetic moments in the film under investigation in a field of 250 Oe, which at $\varphi = 5°$ almost coincides with the coercive force H_c of the sample, is shown at the right of Fig. 1. It should be noted that the total projection of the magnetic moments onto the direction of the magnetization reversal field is close to zero. The domain precursors, i.e., the regions in which magnetic moments of dipoles are almost parallel to each other, are clearly seen in Fig. 1.

It is obvious that the coercive force of the thin-film sample should depend on a specific distribution of directions of the easy magnetization axes in the crystallites forming the magnetic film. It should be noted that the lower the dimension of the film, the larger the scatter in the coercive forces for different random distributions of the easy magnetization axes in its dipoles, which are obtained with the use of a random number generator. This inference is illustrated by the hysteresis loops shown in Fig. 2 for the films with dimensions of 20 × 20 (Fig. 2a) and 200 × 200 dipoles (Fig. 2b). In the study, we chose the hysteresis loops with the minimum (curve *1*), maximum (curve *3*), and average (curve *2*) coercive forces obtained using the numerical calculations for a set of random distributions of the anisotropy axes in the crystallites of the films. The magnetization

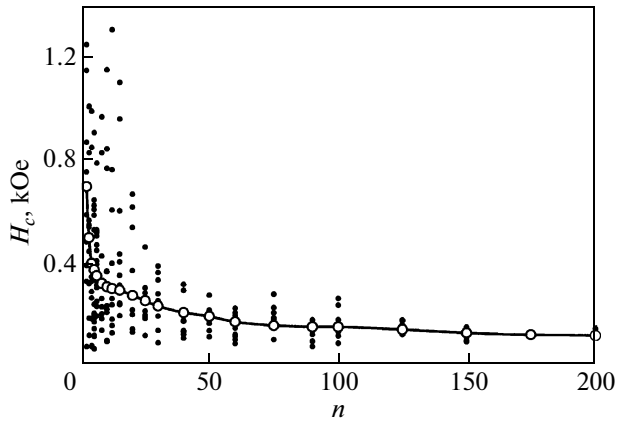

Fig. 3. Dependence of the coercive force on the dimension of the magnetic films for a set of random distributions of anisotropy axes of dipoles (closed circles). Open circles represent averaged values of the coercive forces.

reversal was performed by the planar field directed along one of the sides of the square samples ($\varphi = 0$). It should be noted that the sizes and magnetic parameters of the dipoles were identical to those used in the previous study. It can be seen that an increase in the dimension of the film leads to a decrease in both the average value of the coercive forces and their scatter. This regularity is clearly seen in Fig. 3, in which the closed circles indicate the coercive forces of the monolayer magnetic films with different dimensions that were obtained in each case for ten different random distributions of the anisotropy axes in the crystallites.

Figure 4 illustrates the change in the hysteresis loops for the films with dimensions of 20 × 20 (Fig. 4a) and 50 × 50 nanocrystallites (Fig. 4b) as a function of the dipole–dipole interaction between them. For each variant, the curves were constructed for one fixed random distribution of the anisotropy axes in the case of the absence of the dipole–dipole interaction between nanocrystallites (curve *1*) and in the cases where the dipole–dipole interaction was included to distances equal to two exchange interaction lengths $2R$ (curve *2*) and ten exchange interaction lengths $10R$ (curve *3*). It should be noted that hysteresis loops *3* for the film structures under investigation remain almost unchanged with a further increase in the distance at which the dipole–dipole interaction is taken into account. For convenience of comparison, the sizes and all magnetic parameters of the nanocrystallites were identical to those used in the previous investigation. It can be seen that the occurrence of the dipole–dipole interaction between the crystallites in the film hinders the magnetization reversal, which leads to an increase in both the coercive force and the saturation field. It should also be noted that, with an increase in the dimension of the film, the dependence of the coercive force on the dipole–dipole interaction rapidly weakens, whereas the dependence of the saturation field remains almost the same.

Figure 5 shows the change in the hysteresis loops for the films with dimensions of 20 × 20 (Fig. 5a) and 50 × 50 dipoles (Fig. 5b) as a function of the uniaxial magnetic anisotropy. The curves were also constructed for one fixed variant of the random distributions of the anisotropy axes in the crystallites with allowance made for the dipole–dipole interaction between them to the distance $8R$. Moreover, the magnetic characteristics and sizes of nanoparticles remained unchanged and the anisotropy fields in the crystallites were as follows: 0.1 (curve *1*), 4.0 (curve *2*), and 6.0 kOe (curve *3*). As

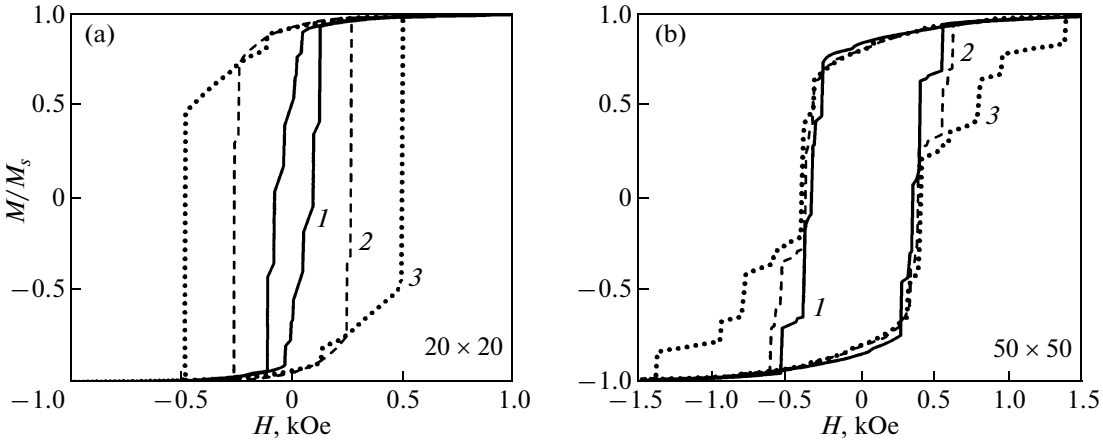

Fig. 4. Hysteresis loops constructed for the films with dimensions of (a) 20 × 20 and (b) 50 × 50 dipoles with the use of one random distribution of anisotropy axes in particles (*1*) in the absence of the dipole–dipole interaction between them and with due regard for the dipole–dipole interaction at distances up to (*2*) $2R$ and (*3*) $10R$.

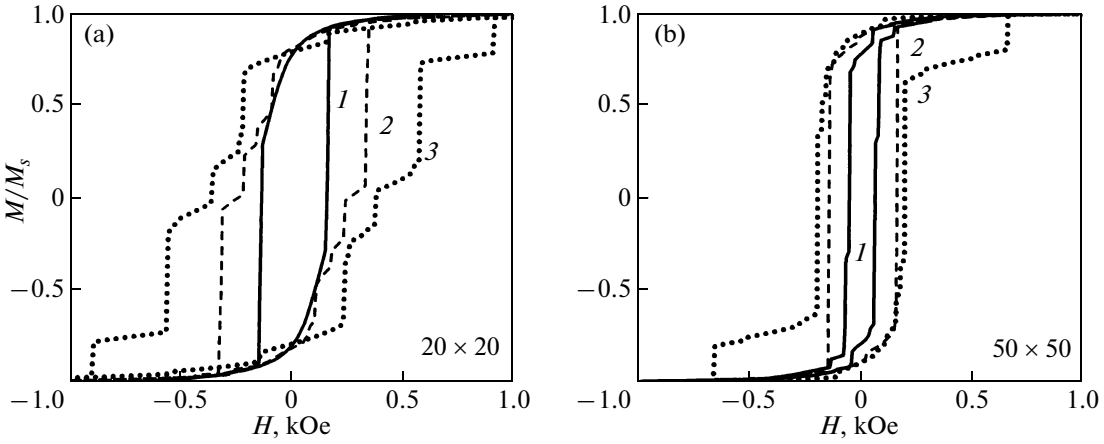

Fig. 5. Hysteresis loops constructed for the films with dimensions of (a) 20 × 20 and (b) 50 × 50 dipoles with the use of one chosen variant of the random distributions of anisotropy axes in crystallites for dipoles with anisotropy fields of (*1*) 0.1, (*2*) 4.0, and (*3*) 6.0 kOe.

could be expected, an increase in the anisotropy field leads a monotonic increase not only in the coercive force but also in the saturation field of the samples and this regularity manifests itself irrespective of the dimension of the films. Furthermore, the performed simulation showed that an increase in the dimension of the structure results in a rapid decrease in both the coercive force and the saturation field.

The dependence of the coercive force on the linear size of crystallite grains d that form the monolayer magnetic film with a dimension of 50 × 50 dipoles is plotted in Fig. 6. As before, the calculations were carried out under the assumption that the anisotropy field of the individual dipole is $H_k = 3.5$ kOe, its saturation magnetization is $M_s = 1250$ G, and the exchange constant is $A = Jd^2 = 5 \times 10^{-7}$ erg/cm. The dipole–dipole interaction between the particles was taken into account to the distance equal to eight exchange correlation lengths. It can be seen from Fig. 6 that the coercive force increases with an increase in the size d; however, the coercive force remains almost unchanged in the range $d < 2$ nm and in the range $d > 20$ nm, where the coercive force H_c reaches saturation. This behavior of the coercive force is associated with the fact that the strong but "short-range" exchange interaction aligns the magnetic moments of all dipoles in parallel to each other only in the case where their sizes are considerably smaller than the correlation length. In this case,

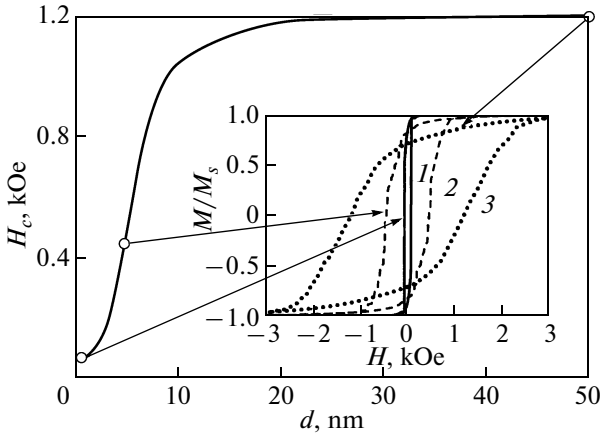

Fig. 6. Dependence of the coercive force on the size of crystallites in the film with a dimension of 50 × 50. The inset shows the hysteresis loops for d = (*1*) 1, (*2*) 5, and (*3*) 50 nm.

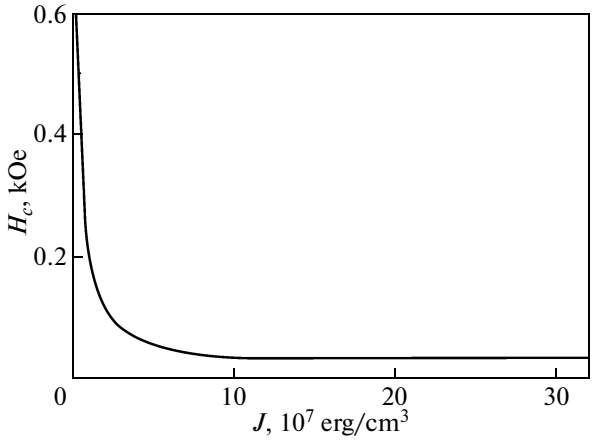

Fig. 7. Dependence of the coercive force on the exchange interaction constant for the film with a dimension of 50 × 50.

the scatter of the directions of the anisotropy axes of all dipoles located in the region of the exchange interaction, in essence, levels the crystallographic anisotropy of this region. That is why, not only the coercive force in the magnetization reversal in any direction but also the saturation field are small in nanocrystalline and "X-ray amorphous" magnetic films [1]. This inference is confirmed by the hysteresis loop shown by line *1* constructed in Fig. 6 for the film with the crystallite sizes $d = 1$ nm. The investigations revealed that an increase in the crystallite size d leads to the simultaneous increase in both the coercive force and the saturation field.

The study of the behavior of the magnetic characteristics of the samples by varying the exchange interaction between the nanoparticles in the film under consideration demonstrated that the coercive force and the saturation field of the samples rapidly decrease with an increase in the exchange interaction constant J but only in the initial range $0–2 \times 10^7$ erg/cm^3 (Fig. 7). A further increase in the exchange interaction results in saturation of these characteristics at $J > 3 \times 10^7$ erg/cm^3. In this investigation, the sizes of the crystallites in the magnetic film were fixed $d = 2.5$ nm, it was assumed that the anisotropy field of the individual dipole is $H_k = 3.5$ kOe and its saturation magnetization is $M_s = 1250$ G, and the dipole–dipole interaction between the particles was taken into account to the distance equal to eight exchange correlation lengths.

4. CONCLUSIONS

Thus, a new approach has been proposed for determining an equilibrium configuration of magnetic moments in a discrete model of a ferromagnet. It has been demonstrated that this problem can be reduced to the problem of linear algebra and can be solved using the developed numerical algorithms, which makes it possible to simulate systems with a large number of interacting dipoles. This allows one to use the effective algorithms for manipulating with sparse matrices by ignoring the dipole–dipole interaction of magnetic moments in the model or with its partial inclusion, as well as parallel calculations when solving large-scale problems on multiprocessor systems.

In order to solve the formulated linear problem, we have proposed a relatively simple numerical algorithm, which represents a modification of the known power method used for solving the partial eigenvalue problem. The efficiency of the method and validity of the solutions obtained is confirmed by good agreement between the results of our calculations and the calculations previously performed in [9] in the numerical simulation of the equilibrium distribution of magnetic moments in a thin nanocrystalline film with a random distribution of anisotropy axes in grains.

The developed numerical calculations make it possible to investigate not only the magnetic microstructure of thin-film samples formed by dipoles of nanocrystalline sizes but also to obtain the hysteresis loops for different orientations of the magnetic field and to study the magnetization reversal processes in films. In this work, we have investigated the main regularities of the magnetization reversal in square monolayer nanocrystalline films. Moreover, we have studied the behavior of the coercive force by varying the uniaxial magnetic anisotropy field, the exchange and dipole–dipole interaction energies, the nanocrystallite size, and the dimension n of the samples. The possibility of observing the processes of the formation of domains and domain walls has been clearly demonstrated for the samples under investigation.

It is important to note that the finished program for analyzing the micromagnetic structure of nanocrystalline objects has a convenient interface and, in principle, allows one to investigate not only film materials but also bulk materials with an arbitrary dimension in three directions. This provides a possibility of studying the influence of demagnetizing fields of the sample itself on the processes of its magnetization reversal.

ACKNOWLEDGMENTS

This study was supported by the Council on Grants from the President of the Russian Federation (grant no. 3818.2008.3), the Siberian Branch of the Russian Academy of Sciences (integration project no. 5), the Presidium of the Russian Academy of Sciences (project no. 27.1), and the Ministry of Education and Science of the Russian federation (state contract nos. 02.740.11.0220 and 02.740.11.0568.

REFERENCES

1. B. A. Belyaev, A. V. Izotov, S. Ya. Kiparisov, and G. V. Skomorokhov, Fiz. Tverd. Tela (St. Petersburg) **50** (4), 650 (2008) [Phys. Solid State **50** (4), 676 (2008)].
2. W. Scholz, D. Suess, T. Schrefl, and J. Fidler, J. Appl. Phys. **95**, 6807 (2004).
3. R. P. Boardman, H. Fangohr, M. J. Fairman, J. Zimmermann, S. J. Cox, A. A. Zhukov, and P. A. J. de Groot, J. Magn. Magn. Mater. **312**, 234 (2007).
4. M. Kisielewski, A. Maziewski, V. Zablotskii, and W. Stefanowicz, Physica B (Amsterdam) **372**, 316 (2006).
5. O. Nedelko, P. Didukh, and A. Slawska-Waniewska, J. Magn. Magn. Mater. **254–255**, 281 (2003).
6. E. O. Kamenetskii, Phys. Rev. E: Stat., Nonlinear, Soft Matter Phys. **63**, 066612 (2001).

7. M. Grimsditch, L. Giovannini, F. Monotcello, F. Nizzoli, G. K. Leaf, and H. G. Kaper, Phys. Rev. B: Condens. Matter **70**, 054409 (2004).

8. K. Rivkin, L. E. DeLong, and J. B. Ketterson, J. Appl. Phys. **97**, 10E309 (2005).

9. D. S. Il'yushchenkov, V. I. Kozub, and I. N. Yassievich, Fiz. Tverd. Tela (St. Petersburg) **49** (10), 1853 (2007) [Phys. Solid State **49** (10), 1944 (2007)].

10. S. V. Kolmogortsev and R. S. Iskhakov, Fiz. Tverd. Tela (St. Petersburg) **47** (3), 480 (2005) [Phys. Solid State **47** (3), 495 (2005)].

11. K. Rivkin and J. B. Ketterson, J. Magn. Magn. Mater. **306**, 204 (2006).

12. K. Rivkin, A. Heifetz, P. R. Sievert, and J. B. Ketterson, Phys. Rev. B: Condens. Matter **70**, 184410 (2004).

13. M. J. Donahue and D. G. Porter, Interagency Report No. 6376, NISTIR (National Institute of Standards and Technology, Gaithersburg, Maryland, United States, 1999).

14. W. Scholz, J. Fidler, T. Schrefl, D. Suess, R. Dittrich, H. Forster, and V. Tsiantos, Comput. Mater. Sci. **28**, 366 (2003).

15. P. M. Morse and H. Feshbach, *Methods of Theoretical Physics* (McGraw-Hill, New York, 1953; Inostrannaya Literatura, Moscow, 1958), Vol. 1.

16. G. H. Golub and Ch. F. van Loan, *Matrix Computations* (Johns Hopkins University Press, Baltimore, Maryland, United States, 1996; Mir, Moscow, 1999).

17. A. V. Izotov and B. A. Belyaev, Izv. Vyssh. Uchebn. Zaved., Fiz. **51** (9/2), 180 (2008).

Translated by O. Borovik-Romanova